

# Extrinsic inhomogeneity effects in magnetic, transport and magnetoresistive properties of $\text{La}_{1-x}\text{Ca}_x\text{MnO}_3$ ( $x \approx 0.33$ ) crystal prepared by the floating zone method

B. I. Belevtsev<sup>a,\*</sup>, D. G. Naugle<sup>b</sup>, K. D. D. Rathnayaka<sup>b</sup>,  
A. Parasiris<sup>b</sup>, J. Fink-Finowicki<sup>c</sup>

<sup>a</sup>*B. Verkin Institute for Low Temperature Physics and Engineering, National Academy of Sciences, Kharkov, 61103, Ukraine*

<sup>b</sup>*Texas A&M University, College Station, TX 77843, USA*

<sup>c</sup>*Institute of Physics, Polish Academy of Sciences, 32/46 Al. Lotnikow, 02-668 Warsaw, Poland*

---

## Abstract

The magnetic, transport and magnetoresistive properties of  $\text{La}_{1-x}\text{Ca}_x\text{MnO}_3$  ( $x \approx 0.33$ ) crystals prepared by the floating-zone method are studied. In general, these properties testify to rather good crystal perfection of the sample studied. In particular, a huge magnetoresistance ( $[R(0) - R(H)]/R(H)$  in the field  $H = 5$  T is about  $\approx 2680$  %) is found near the Curie temperature (216 K). At the same time, some distinct features of measured properties indicate the influence of extrinsic inhomogeneities arising due to technological factors in the sample preparation. Analysis of the data obtained shows that these are rare grain boundaries and twins.

*Key words:* manganites, colossal magnetoresistance, magnetically ordered materials, magnetic inhomogeneities

*PACS:* 75.47.Gk; 75.47.Lx

---

## 1 Introduction

The structural, magnetic and electron transport properties of mixed-valence manganites of the type  $\text{R}_{1-x}\text{A}_x\text{MnO}_3$  (where R is a rare-earth element, A a

---

\* Corresponding author. Email address: belevtsev@ilt.kharkov.ua. Fax: ++380-572-335593. Phone: ++380-572-308563.

divalent alkaline-earth element) attracted much attention in the scientific community in the last decade (see reviews [1,2,3,4,5,6]). The interest is caused by observation of huge negative magnetoresistance (MR) near the Curie temperature,  $T_c$ , of the paramagnetic-ferromagnetic transition for manganites with  $0.2 \leq x \leq 0.5$ . This phenomenon called “colossal” magnetoresistance (CMR), is expected to have application in advanced technology. The unique properties of mixed-valence manganites are determined by the complex spin, charge and orbital ordered phases, and, therefore, are of great fundamental interest for physics of strongly correlated electrons. At present, it is believed that one of the key features of manganites is their intrinsic inhomogeneities in the form of coexisting, competing ferromagnetic and antiferromagnetic/paramagnetic phases [3,4,6]. This phenomenon is generally called “phase separation”. The known experimental studies give numerous (but predominantly indirect) evidence of structural and magnetic inhomogeneities in manganites, but it hardly can be said that they are intrinsic in all cases. The point is that in all manganites extrinsic inhomogeneities are inevitably present (even in single crystal samples). The inhomogeneities of this type arise due to various technological factors in the sample preparation. They can cause chemical-composition inhomogeneity (first of all in the oxygen content), structural inhomogeneities (polycrystalline or even granular structure), strain inhomogeneities and so on. It is easy to find in the literature many experimental studies in which finding of phase separation effects is proclaimed, but the interpretations are often doubtful. In such cases the effects of technological inhomogeneities are quite obvious or, at least, cannot be excluded.

The experimental data demonstrate that technological inhomogeneities are unavoidable for any preparation method [7]. For this reason, in many cases it is better to speak about multiphase coexistence instead of the phase separation. It is quite reasonable, therefore, that consideration of experimental data for mixed-valence manganites and development of theoretical models for them take into account the unavoidable influence of extrinsic disorder and inhomogeneity. These inhomogeneities can act separately as well as together with the intrinsic inhomogeneities (phase separation) and determine to a great extent the magnetic and magnetotransport properties of these compounds.

In this article we present a study of structure, magnetic, and magnetoresistive properties of crystals with nominal composition  $\text{La}_{0.67}\text{Ca}_{0.33}\text{MnO}_3$  prepared by the floating zone method. The measured properties generally indicate that the sample studied is of rather high crystal perfection. At the same time some features of the transport properties reflect the essential influence of extrinsic structural inhomogeneities arising due to technological factors in the sample preparation.

## 2 Experimental

Crystals of nominal composition  $\text{La}_{0.67}\text{Ca}_{0.33}\text{MnO}_3$  were grown by the floating zone method at the Institute of Physics, Warsaw. The appropriate amounts of starting materials  $\text{La}_2\text{O}_3$ ,  $\text{CaCO}_3$  and  $\text{MnO}_2$  were calcined at  $1000^\circ\text{C}$ , then mixed, compacted into pellets and sintered at  $1400^\circ\text{C}$ . Subsequently, the pellets were milled, and the resulting powder was then pressed to form the feed rod with a diameter of 8 mm and a length of 90 mm. This rod was further sintered at  $1470^\circ\text{C}$  for 12 h in air. An optical furnace (type URN-2-3Pm made by Moscow Power Engineering Institute) with two ellipsoidal mirrors and a 2500 W xenon lamp as the heat source was used for crystallization. The feed rod and the growing crystal were rotated in opposite directions to make heating uniform and to force convection in the melting zone. The growth rate was 1 mm/h. An additional afterheater was used for lowering the temperature gradients in the growing crystal.

As shown by previous experience [8], manganite crystals produced by this technique are almost single crystals, and, in this respect, they have far better crystal quality and far less porosity than samples prepared by a solid-state reaction technique. On the other hand, the crystals have twin domain structure and may have a few grain boundaries. This question will be discussed more thoroughly below.

The disc-shaped sample for investigation was cut from the middle part of the cylindrical crystal (about 8 mm in diameter). It is known [9,10] that  $\text{La}_{1-x}\text{Ca}_x\text{MnO}_3$  crystals grown by the floating zone technique have an inhomogeneous distribution of La and Ca along the growth direction. The initial part of the crystal is usually somewhat enriched in La and depleted in Ca. The microprobe elemental analysis has shown that the sample studied has a chemical composition close to the nominal one. This is supported by its transport and magnetic properties as well, as described below. The sample characterization and measurements were done by a variety of experimental techniques. Crystal structure was determined by the X-ray diffraction (XRD) method. The XRD spectra (from powders and bulk pieces taken from the crystal) were obtained using a Rigaku model D-MAX-B diffractometer with a graphite monochromator and  $\text{Cu } K_{\alpha 1,2}$  radiation. The ac susceptibility and dc magnetization were measured in a Lake Shore model 7229 Susceptometer/Magnetometer. Resistance as a function of temperature and magnetic field was measured using a standard four-point probe technique in magnetic fields up to 5 T.

### 3 Results and discussion

#### 3.1 X-ray diffraction study

Bulk  $\text{La}_{1-x}\text{Ca}_x\text{MnO}_3$  has a distorted perovskite structure, which is believed to be orthorhombic below about 750 K [5,11,12,13,14]. The deformation of the cubic perovskite lattice is determined by rotation of  $\text{MnO}_6$  octahedra and the Jan-Teller distortion [5,14]. For the concentration range  $0.25 < x < 0.5$ , Jan-Teller distortion is found to be negligible [12,14]. In the orthorhombic space group  $Pnma$ , lattice constants are  $a \approx \sqrt{2} a_p$ ,  $b \approx 2a_p$ , and  $c \approx \sqrt{2} a_p$ , where  $a_p$  is the lattice constant of the pseudo-cubic perovskite lattice. The symmetry of distortions is, however, still a matter of some controversy [15]. In some studies a monoclinic lattice is found [15,16]. Generally, however, the deviations from cubic symmetry are found to be fairly small, especially in the CMR range ( $0.2 < x < 0.5$ ). Several scientific groups have found only cubic symmetry in this compound with lattice parameter  $a_p$  in the range 0.385-0.388 nm for  $0.2 < x < 0.5$  (see, for example, Refs. [17,18]).

In this study, XRD investigation was used (along with other methods) to judge the crystal perfection and structural homogeneity of the samples. The x-ray spectra from powders and bulk sections of different parts of the crystal were measured. We found that XRD powder patterns from the outer and inner parts of the crystal are quite different. The positions of all intense and well-defined lines for the outer part of the crystal are exactly consistent (within the uncertainty of the XRD recording) with those of perfect cubic perovskite<sup>1</sup>. A lattice constant  $a_p = 0.38713$  nm was computed with the corresponding unit cell volume  $v_p \approx 0.0580$  nm<sup>3</sup>. An application of the Powdercell program [19], which takes into account not only positions, but intensities and profiles of the lines as well, has shown that an orthorhombic  $Pnma$  lattice also corresponds fairly well to the experimental XRD powder pattern. This gives the lattice constants  $a = 0.54849$  nm,  $b = 0.77587$  nm, and  $c = 0.54645$  nm with a unit cell volume  $v_o \approx 0.2322$  nm<sup>3</sup>.

A quite different XRD powder pattern was obtained for inner part of the crystal (Fig. 1). In low resolution this pattern looks the same as that for the outer part of the crystal, but closer inspection shows that most of the lines are split (into two, three, or even four closely located lines). Significant line splitting with a severely distorted cubic perovskite lattice was found previously

---

<sup>1</sup> The typical linewidth (on the half of the magnitude) of the most intensive lines is found to be in the range of 0.3–0.4 degree. The step of the XRD pattern recording was 0.03 degree, that permitted to record surely the line profiles and reveal available line splitting, which was really found in the inner part of the crystal, as it is shown below.

in low doped  $\text{LaMnO}_3$  with  $\text{Mn}^{4+}$  (or Ca) concentration in the range 0-25 % [16], which was attributed to monoclinic distortions. Splitting due to small orthorhombic distortions for the Ca concentration range  $0.25 < x < 0.5$  is usually very narrow, so that it cannot be observed clearly (only some line broadening can be seen) [11,20,21].

The splitting of the Bragg reflections could be also ascribed to twinning, which is quite common in mixed-valence manganites. Origin of twinning in perovskite crystals is well known [14]. At high temperatures (above about  $900^\circ\text{C}$ )  $\text{La}_{1-x}\text{Ca}_x\text{MnO}_3$  ( $0.2 < x < 0.5$ ) has a cubic perovskite lattice [21]. When cooling, the cubic-orthorhombic (or even cubic-monoclinic) transition takes place, during which  $\text{MnO}_6$  octahedra are rotated and distorted [14]. Since different directions of rotation with respect to the original cubic axes are possible, most  $\text{La}_{1-x}\text{Ca}_x\text{MnO}_3$  single crystals are twinned. In this case additional reflections (line splitting) can appear if lattices in twin domains do not coincide. This can take place in the case of monoclinic distortions [14] or owing to other reasons (for example, when inhomogeneous strains are present). It is impossible, however, on the basis of powder diffraction data to see splitting due to twinning [14]. Only special methods of single-crystal x-ray diffraction have opportunities to reveal twinning effects in manganites [14,22]. But the line splitting in a powder XRD pattern due to considerable distortions from the cubic symmetry is quite possible.

We have applied the above-mentioned Powdercell program to the XRD data for inner part of the crystal. Assuming that crystal lattice is orthorhombic, we obtained lattice constants  $a = 0.54972$  nm,  $b = 0.77801$  nm, and  $c = 0.54551$  nm with a unit cell volume  $v_o \approx 0.2332$  nm<sup>3</sup>, but agreement between the calculated and experimental XRD patterns is far worse in this case than that for the outer part of the crystal. It appears therefore that distortions from cubic symmetry are more severe than orthorhombic ones and they can be monoclinic as it was found in some manganites in Refs. [15,16,22]. This suggestion has found a partial support after application of a Monte Carlo program McMaille V3.04 [23] to the experimental XRD data. This has shown rather convincingly that monoclinic lattice is much better corresponds to the XRD data of the inner part of the sample than orthorhombic lattice.

X-ray study with a Laue camera revealed that the XRD pattern of a small piece taken from the central part of the sample corresponds to a single crystal structure. Investigation with an optical microscope has shown, however, that the sample as a whole is not a single crystal but consists of a few grains.

### 3.2 Magnetic properties

Distinctions between the XRD patterns for outer and inner parts of the crystal studied imply that their magnetic properties can be different as well. That is indeed found in this study. The temperature behavior of the ac susceptibility is presented in Fig. 2. It is seen that the magnetic transition from the paramagnetic (PM) to the ferromagnetic (FM) state with decreasing temperature is considerably smeared for the outer part of the crystal indicating that this part is rather disordered. In contrast to this, the magnetic transition in the central part of the sample is fairly sharp, indicating a significant crystal perfection and stoichiometric homogeneity for this part. The same conclusion can be arrived from comparison of the temperature dependences of the dc magnetization,  $M(T)$ , from which only that for central part of the sample is shown in Fig. 3.

Taking  $T_c$  as the temperature of the inflection point in the  $M(T)$  curve, we found that  $T_c \approx 216$  K. Nearly the same value can be obtained if  $T_c$  were defined as the temperature at which  $M$  comes to half of the maximum value. This  $T_c$  value (216 K) is less than that ( $T_c \approx 250$  K) usually found in polycrystalline ceramic samples in  $\text{La}_{1-x}\text{Ca}_x\text{MnO}_3$  with  $0.3 < x < 0.35$ , and which is indicated in the accepted phase diagram for this system [5]. This value agrees, however, well with those found in single crystal samples of the same composition, where  $T_c$  values are usually found to be in the range 216–230 K [24,25,26,27,28], although some rare exceptions are known as well [29].

The inset in Fig. 3 shows the magnetic field dependence of the magnetization at  $T = 10$  K. It is seen that the magnetization is close to saturation above the field  $H \approx 0.3$  T. We have recorded  $M(H)$  dependences for other temperatures as well in the range 4–51 K and at fields up to 9 T. Taking the saturation value of  $M$  (95.3 emu/g) at the highest field (9 T) in low temperature range, we have obtained the magnetic moment per formula unit in the sample studied to be equal to  $\mu_{fu} \approx 3.65 \mu_B$ , where  $\mu_B$  is the Bohr magneton. For the nominal composition  $\text{La}_{1-x}\text{Ca}_x\text{MnO}_3$  ( $x = 0.33$ ) of the sample studied, taking into account that the spin of  $\text{Mn}^{+3}$  is  $S = 2$  and that of the  $\text{Mn}^{+4}$  is  $S = 3/2$ ,  $\mu_{fu}$  should be equal to  $(4 - x) \mu_B$ , that is to  $3.67 \mu_B$ . The value of  $\mu_{fu} \approx 3.65 \mu_B$  obtained provides evidence that the inner part of the sample is close to the nominal composition and does not have any appreciable oxygen deficiency. Since the inner part of the sample appears to be more homogeneous and perfect than the outer part, resistive and magnetoresistive measurements were done for inner part of the sample only.

### 3.3 Resistive and magnetoresistive properties

Temperature dependences of the resistivity,  $\rho$ , and MR,  $\delta_0 = [R(H) - R(0)]/R(0)$ , at different applied fields, are shown in Figs. 4 and 5. Consider first the  $\rho(T)$  behavior (Fig. 4) which appears somewhat complicated. In doing so it is appropriate to take a look at the behavior of the temperature coefficient of resistivity (TCR) [defined as  $(1/R)(dR/dT)$ ] as well. This is presented in Fig. 6. Although the  $\rho(T)$  behavior reflects, generally, a rather high perfection of the crystal studied, some quite distinct features in it should be attributed to the influence of structural and magnetic inhomogeneities. The  $\rho(T)$  curve has two peaks, a sharp one at  $T_p \approx 225$  K, which is near the Curie temperature  $T_c \approx 216$  K, obtained from magnetization and susceptibility studies (Figs. 2 and 3) and a far less pronounced one at  $T_{pin} \approx 190$  K. Additionally,  $\rho(T)$  exhibits two shallow minima, one is situated at  $T'_{min} \approx 201$  K between the two peaks, and another in the low-temperature range at  $T''_{min} \approx 16$  K (see inset in Fig. 4).

Above  $T_c$ , the sample is a PM non-metal with an activated temperature dependence of resistivity, following  $\rho(T) \propto \exp(E_a/T)$ . The activation energy  $E_a$  is found to be equal to 0.09 eV in agreement with that (about 0.1 eV) reported by other authors for single crystal and ceramic samples of  $\text{La}_{1-x}\text{Ca}_x\text{MnO}_3$  ( $x \approx 0.33$ ) [17,24,25,30]. It is known [1,2,3] that the conductivity of Camanganites increases enormously at the transition to the FM state. In the  $\text{La}_{1-x}\text{Ca}_x\text{MnO}_3$  ( $0.2 \leq x \leq 0.5$ ), the PM-FM transition occurs simultaneously with the insulator-metal one. For this reason, the  $\rho(T)$  dependence has a peak at a temperature  $T_p$ . In samples with fairly perfect crystalline structure,  $T_p$  is close to  $T_c$ . This is true to a considerable degree for the sample studied. Other important measures of crystal perfection in manganites are the ratio of the peak resistivity,  $\rho(T_p)$ , and the residual resistivity at low temperature,  $\rho(0)$ . The value of  $\rho(T_p)/\rho(0)$  is about 200 for the sample studied. This is a high value, comparable with that of single crystals and epitaxial films of the best quality [2,24,25,30,31,32]. For ceramic samples, prepared by the solid-state reaction method, the ratio  $\rho(T_p)/\rho(0)$  is usually far less (see Refs. [5,17,18]). It is well known that samples prepared by the floating-zone method generally have a much sharper resistive transition on going from the PM to FM state than is observed for manganite films (compare data in Refs. [2,24,25,30,31,32]). This is so indeed in the sample studied which has an extremely sharp resistive transition near  $T_c$  (Fig. 4). This can be further illustrated by the temperature behavior of TCR (Fig. 6). The highest value of TCR near  $T_c$  found in this study is about 38 %/K; whereas, no more than about 10 %/K is found in the best quality  $\text{La}_{1-x}\text{Ca}_x\text{MnO}_3$  ( $x \approx 0.3$ ) films [32,33].

Along with general characteristics indicating a rather good crystal perfection, the  $\rho(T)$  behavior reveals, at the same time, some features which are deter-

mined by sample inhomogeneities (structural and magnetic). These are the second resistance peak at  $T_{pin} \approx 190$  K and the shallow resistance minimum in the low-temperature range. Consider possible reasons for this behavior. It is believed presently that the PM-FM transition in  $\text{La}_{1-x}\text{Ca}_x\text{MnO}_3$  is of first order at  $0.25 < x < 0.4$  (see Ref. [7] and references therein). It is found as well that FM clusters are present well above  $T_c$  while some PM insulating clusters can persist down to a range far below  $T_c$ . This implies that the PM-FM transition has a percolative character. With decreasing temperature, the PM volume fraction decreases and that of the FM fraction increases. Since the PM phase is insulating and the FM one is metallic, some kind of insulator-metal transition takes place near  $T_c$ . The temperature  $T_p$  corresponds to the situation when metallic FM clusters have merged together in a sufficient degree to ensure a decrease in resistance with further temperature decrease. This temperature indicates a transition from the insulating to the metallic state and, therefore, is called conventionally the temperature of the insulator-metal transition. Below  $T_p$ , the volume of the PM phase continues to decrease with temperature causing a further resistivity decreasing. The temperature width of this type of transition depends in crucial way on the sample extrinsic inhomogeneities induced by various technological factors during the sample preparation (see Sec. 1 and Ref. [7]). In samples, prepared by the floating-zone method, these inhomogeneities are determined by mosaic blocks, twins, inhomogeneous strains, and stoichiometric disorder. These defects are present even in single-crystal Ca-manganites [9,14,34].

Double-peaked (or shouldered)  $\rho(T)$  curves similar to that shown in Fig. 4 were often seen in polycrystalline manganite samples [30,35,36,37,38]. In all cases this behavior was quite reasonably attributed to the influence of grain boundaries. The evident idea is that regions near the grain boundaries are disordered and even depleted in charge carriers compared with that inside the grains [37,38]. This was supported by direct experiments [39,40], which have shown that grain boundary regions (with thickness of the order 10 nm) have a smaller  $T_c$  than that in the core of the grain. For this reason, when the cores of the grains become FM below  $T_c$ , the grain boundary regions still remain in the paramagnetic, insulating state, presenting barriers to the transport current. This prevents the formation of an infinite FM cluster and causes an increase in resistance with decreasing temperature when the FM transition in cores of the grains is completed. The further decrease in temperature, however, leads to a reduction of magnetic disorder in the grain-boundary regions, eliminating some insulating barriers. If this process proceeds sufficiently,  $\rho(T)$  behavior becomes metallic again with the result that a second peak (or shoulder) appears in  $\rho(T)$ . This peak indicates the appearance of the infinite FM cluster.

The second peak at  $T = T_{pin}$  in  $\rho(T)$  curve (Fig. 4) suggests the presence of some grain-boundary-like inhomogeneities in the crystal studied. As a result the  $\rho(T)$  dependence shown in Fig. 4 reflects actually two resistive transitions

in the sample studied. The first is connected with PM-FM transition inside the grains, while the second one signifies the magnetic ordering of grain-boundary regions. On that ground the second peak position at  $T = T_{pin} \approx 190$  K can be taken as a rough estimate of the Curie temperature  $T_{cg}$  of the intergrain regions.

It should be noted that for weak intergrain connectivity (as often takes place in ceramic samples) the second resistance peak can be rather large and even higher than the first peak (caused by the intragrain FM transition) [35,38]. Since the second peak is rather weak for the sample studied, it can be said that grain-boundary-like inhomogeneities are not as strong in it as in ceramic samples. What can be the sources of such inhomogeneities in samples prepared by the floating-zone method? First of all, some rare grain boundaries cannot be excluded in this type of sample [30]. But the major reason is that these samples contain inevitably mosaic blocks and twin domains [14,34]. Twin boundaries act effectively in the same way as grain boundaries, presenting tunnel barriers [34]. The twins are present even in polycrystalline manganites prepared by the solid-state reaction method, where large enough grains (a few microns in size) contain multiple twins [41].

If the second peak in  $\rho(T)$  is determined by the grain-boundary-like interlayers with Curie temperature different from that inside the grains, it must be depressed by an applied magnetic field. This really occurs (see Fig. 4). At the same time no visible features associated with grain boundaries can be seen in the  $M(T)$  dependence (Fig. 3). This is reasonable if the volume fraction of the grain boundaries is sufficiently small.

When the FM transition in grain/twin boundary regions is completed, the boundaries can still exert an influence on the sample conductivity. These boundary regions are places of not only magnetic, but also structural disorder, where charge carriers can be scattered. What's more, grain boundaries appear as natural places for FM domain boundaries. On the basis of the known experimental data [39,40] the following model of grain boundaries in the manganites can be assumed. A transition region between any two grains consists of two layers depleted of charge carriers (and having a reduced Curie temperature  $T_{cg}$ ) and some thin (thickness about a nanometer) insulating layer between them. The latter presents the tunnel barriers for the charge carriers even at low temperature  $T < T_{cg}$  when the two depleted layers become ferromagnetic and, most likely, metallic. It is quite reasonable to assume that the thickness of the insulating layers (tunnel barriers) is not the same throughout the sample, so the system is percolating in this context as well.

Quantum tunneling of the charge carriers occurs between states of equal energy. Actually, however, there is always some energy level mismatch between states in neighboring grains for different reasons. In this case, a charge carrier

should gain some energy (for example, from phonons) to accomplish tunneling. The intergrain conductivity is conditioned, therefore, by the two processes: the tunneling and thermal activation. If the activation energy of tunneling,  $E_t$ , is rather low, then tunneling at high enough temperature,  $kT > E_t$ , is non-activated. In that event the system behaves like a metal ( $dR/dT > 0$ ). Since the grain boundary thickness is not the same throughout the system, the conductivity is percolating. It is determined by the presence of “optimal” chains of grains with maximum probability of tunneling for adjacent pairs of grains forming the chain. These “optimal” chains have some weak links (high-resistance tunnel junctions). At low enough temperature the relation  $kT < E_t$  can become true for such links, and, hence, the measured conductivity of the system will become activated. This is an evident reason for the observed resistance minimum at  $T''_{min} \approx 16$  K (Fig. 4). More generally it can be said that the minimum is determined by competition between the intragrain conductivity and the intergrain tunneling. The low-temperature resistance minimum is typical for systems of FM regions with rather weak interconnections. It has been observed in polycrystalline [42] and even single crystal [34] samples. We found that an applied magnetic field has no noticeable effect on the resistance minimum position. This may signify that the tunnel barriers are non-magnetic in the low temperature range.

It follows from discussion above that the double-peaked feature and the low-temperature resistance minimum in  $\rho(T)$  of the sample studied can be adequately explained by the influence of the grain/twin boundaries. The measured temperature dependences of MR (Fig. 5) reflect the influence of these structural inhomogeneities as well. Generally, the MR in manganites is determined by intrinsic and extrinsic causes. The CMR is an intrinsic effect determined by the ability of an external magnetic field to increase the magnetization. It is clear that at low temperature ( $T \ll T_c$ ) when all spins are already aligned by the exchange interaction, this ability is minimal. The possibility to strengthen the magnetic order with an external magnetic field increases profoundly near  $T_c$  where the magnetic order becomes weaker. For this reason, CMR is maximal near  $T_c$  and goes to nearly zero value for  $T \ll T_c$ . This behavior is unique to bulk or film manganites of rather good crystal perfection [30,33]. The presence of extrinsic inhomogeneities (such as grain boundaries) gives rise to an extrinsic MR effect. Considering Fig. 5, it is safe to assume that the sharp MR peak at  $T \approx 220$  K is caused by CMR; whereas, the rather weak peak at  $T \approx 173$  K is connected with the influence of grain/twin boundaries. The measured temperature behaviors of the MR (Fig. 5) and the resistance (Fig. 4) are clearly correlated and both of them reflect the influence of extrinsic inhomogeneities. At the same time, they also demonstrate the good crystal perfection of the sample. Really, the maximum value of MR, expressed as  $\delta_0 = [R(H) - R(0)]/R(0)$ , is about -96.4 % near the Curie temperature in a 5 T field. This is the CMR indeed. Since  $\delta_0$ , by definition, cannot be higher than 100 %, another characterization of CMR, namely,  $\delta_H = [R(0) - R(H)]/R(H)$

is frequently used. In the crystal studied, the maximum  $\delta_H$  in the 5 T field is about  $\approx 2680$  %. This is even higher than the MR found in some single-crystal Ca-manganites of the nearly same chemical composition (see Ref. [25]). In ceramic samples, however, the values of  $\delta_H$  are usually about two orders of the magnitude less [17,35,39].

It is known that a contribution to MR coming from grain-boundary-like inhomogeneities increases with decreasing temperature. Discussion of the possible mechanisms for this extrinsic type of the MR can be found in Refs. [43,44,45,46]. The sample studied does indeed show a continuous increase in MR with decreasing temperature in a 0.5 T field in the temperature range below 200 K (Fig. 5). In higher fields, the MR behavior is more complicated. It should be noted that the temperature behavior of MR and its changes with increasing applied magnetic field, revealed in the sample studied (Fig. 5), are quite similar to that found in Ref. [30] for the MR of *a single grain boundary* in a Ca-manganite crystal grown by the floating-zone method. This suggests once again that grain/twin boundaries in the sample studied are not large in number.

It is well established [43,44,45,46,47] also that the extrinsic MR connected with grain boundaries has one more characteristic feature. In the low-field region ( $H < H_s$ , where  $H_s$  is a characteristic field) the resistance decreases rapidly with increasing  $H$  [so called, low-field MR (LFMR)]. For  $H > H_s$ , the resistance changes more gradually [high-field MR (HFMR)]. In both these field regions, the resistance changes almost linearly with  $H$ . The LFMR is found to decrease rather rapidly with increasing temperature so that the broken-line type of the  $R(H)$  dependence is changed to a smooth featureless dependence for higher temperature. All these features of extrinsic MR can be seen in Fig. 7, where MR *vs*  $H$  for two temperatures (4.2 K and 68 K) is presented. In the known studies of manganites the characteristic field  $H_s$  is typically below 0.5 T and is attributed to the field of magnetic domain rotation (when the magnetization magnitude comes close to the technical saturation value). This corresponds roughly to the dependence of  $M(H)$  shown in the inset to Fig. 3.

It is currently believed [44,46,47] that the grain-boundary MR in manganites is determined primarily by the spin-dependent tunneling of charge carriers between the grains. The LFMR is attributed to magnetic alignment of the grains; whereas, HFMR to an increase in the spontaneous magnetization in higher field. For the low temperature range the latter process occurs mainly within the disordered grain-boundary regions, while for high enough temperature it takes place mainly inside the grains causing CMR. This competition of CMR and the extrinsic MR gives a somewhat intricate picture of the total MR behavior found in this study. We will not consider further these or other peculiarities of the extrinsic MR connected with grain-boundary-like inhomogeneities nor the corresponding possible mechanisms of this behavior.

It is clear enough from the data obtained that the sample studied contains inhomogeneities of this type.

In conclusion, we have studied structure, magnetic, and magnetoresistive properties of crystals with nominal composition  $\text{La}_{0.67}\text{Ca}_{0.33}\text{MnO}_3$  prepared by the floating zone method. The properties indicate undoubtedly that the sample is of fairly high crystal perfection. In particular, it has very low resistivity at low temperature and a huge MR near the Curie temperature ( $\delta_H = [R(0) - R(H)]/R(H)$  in the field  $H = 5$  T is about  $\approx 2680$  %). At the same time, some features of the transport and magnetoresistive properties reflect the essential influence of extrinsic grain-boundary type structural inhomogeneities arising due to technological factors in the sample preparation. It is shown that these inhomogeneities are rare grains and twins.

The work at TAMU was supported by the Robert A. Welch Foundation, Houston, Texas (Grant A-0514) and the National Science Foundation (DMR-0111682 and DMR-0422949). B. I. B. acknowledges support from Program “Nanostructural systems, nanomaterials, nanotechnologies” of the National Academy of Sciences of Ukraine under grant No. 3-026/2004.

## References

- [1] A. P. Ramirez, J. Phys.: Condens Matter 9 (1997) 8171.
- [2] J. M. D. Coey, M. Viret, and S. von Molnar, Adv. Phys. 48 (1999) 167.
- [3] E. Dagotto, T. Hotta, and A. Moreo, Phys. Rep. 344 (2001) 1.
- [4] E. L. Nagaev, Phys. Uspekhi 39 (1996) 781; Phys. Rep. 346 (2001) 387.
- [5] K.H. Kim, M. Uehara, V. Kiryukhin, and S-W. Cheong, in *Colossal magnetoresistive manganites*, T. Chatterji (ed.), Kluwer Academic Publ., Dordrecht, Netherlands (2003); preprint cond-mat/0212113.
- [6] E. Dagotto, J. Burgu, and A. Moreo, Solid State Commun. 126 (2003) 9; E. Dagotto, preprint cond-mat/0302550.
- [7] B. I. Belevtsev, Fiz. Nizk. Temp. 30 (2004) 563 [Low Temp. Phys. 30 (2004) 421]; preprint cond-mat/0308571.
- [8] B. I. Belevtsev, A. Ya. Kirichenko, N. T. Cherpak, G. V. Golubnichaya, I. G. Maximchuk, E. Yu. Beliayev, A. S. Panfilov, J. Fink-Finowicki, J. Magn. Magn. Mater. 281 (2004) 97; preprint cond-mat/0404131.
- [9] D. Shulyatev, S. Karabashev, A. Arsenov, Ya. Mukovskii, and S. Zverkov, J. Cryst. Growth 237-239 (2002) 810.
- [10] Ya. M. Mukovskii, Rossiiskii Khim. Zh. (Russian Chem. Journ.) XLV (2001) 32.
- [11] P. Dai, Jiandi Zhang, H. A. Mook, S.-H. Liou, P. A. Dowben, and E. W. Plummer, Phys. Rev. B 54 (1996) R3694.
- [12] S. J. Hibble, S. P. Cooper, A. C. Hannon, I. D. Fawcett, and M. Greenblatt, J. Phys.: Cond. Matter 11 (1999) 9221.
- [13] A. Das, K. R. Chakraborty, S. S. Gupta, S. K. Kulshreshtha, and S. K. Paranjpe, J. Magn. Magn. Mater. 237 (2001) 41.
- [14] Bas B. Van Aken, A. Meetsma, Y. Tomioka, Y. Tokura, and Thomas T. M. Palstra, Phys. Rev. B 66 (2002) 224414; B.B. Van Aken, Ph.D. Thesis, University of Groningen (2001), [www.ub.rug.nl/eldoc/dis/science](http://www.ub.rug.nl/eldoc/dis/science).
- [15] O. I. Lebedev, G. Van Tendeloo, A. M. Abakumov, S. Amelinckx, B. Leibold, and H.-U. Habermeyer, Phil. Mag. A 79 (1999) 1461.
- [16] E. O. Wollan and W. C. Koehler, Phys. Rev. 100 (1955) 545.
- [17] R. Mahendiran, S. K. Tiwary, A. K. Raychaudhuri, T. V. Ramakrishnan, R. Manesh, N. Rangavittal, and C. N. R. Rao, Phys. Rev. B 53 (1996) 3348.
- [18] R. Laiho, K. G. Lizunov, E. Lähderanta, P. Petrenko, V. N. Stamov, and V. S. Zakhvalinskii, J. Magn. Magn. Mater. 213 (2000) 271.

- [19] Available at <http://www.ccp14.ac.uk>.
- [20] Y. H. Li, K. A. Thomas, P. S. I. P. N. de Silva, L. F. Cohen, A. Goyal, M. Rajeswari, N. D. Mathur, M. G. Blamire, J. E. Evetts, T. Venkatesan, and J. L. MacManus-Driscoll, *J. Mater. Res.* **13** (1998) 2161.
- [21] Jiaqing He, Renhui Wang, Jiaian Gui, and Cheng Dong, *Phys. Stat. Sol. B* **229** (2002) 1145.
- [22] R. Tamazyan, Sander van Smaalen, A. Arsenov, and Ya. Mukovskii, *Phys. Rev. B* **66** (2002) 224111.
- [23] Available at <http://www.cristal.org/mcmaille>.
- [24] S. H. Chun, M. B. Salamon, Y. Tomioka, and Y. Tokura, *Phys. Rev. B* **61** (2000) R9225.
- [25] Y. Lyanda-Geller, S. H. Chun, M. B. Salamon, P. M. Goldbart, P. D. Han, Y. Tomioka, A. Asamitsu, and Y. Tokura, *Phys. Rev. B* **63** (2001) 184426.
- [26] Chang Seop Hong, Wan Seop Kim, and Nam Hwi Hur, *Phys. Rev. B* **63** (2001) 092504.
- [27] H. S. Shin, J. E. Lee, Y. S. Nam, H. L. Ju, and C. W. Park, *Solid State Commun.* **118** (2001) 377.
- [28] Sheng-Bo Tian, Manh-Huong Phan, Seong-Cho Yu, and Nam Hwi Hur, *Physica B* **327** (2003) 221.
- [29] C. P. Adams, J. W. Lynn, V. N. Smolyaninova, A. Biswas, R. L. Greene, W. Ratcliff II, S-W. Cheong, Y. M. Mukovskii, and D. A. Shulyatev, preprint cond-mat/0304031.
- [30] B. Vertruyen, R. Cloots, A. Rulmont, G. Dhalenne, M. Ausloos, and Ph. Vanderbemden, *J. Appl. Phys.* **90** (2001) 5692.
- [31] F. Martin, G. Jakob, W. Westerburg, and H. Adrian, *J. Magn. Magn. Mater.* **196-197** (1999) 509.
- [32] A. Goyal, M. Rajeswari, R. Shreekala, S. E. Lofland, S.M. Bhagat, T. Boettcher, C. Kwon, R. Ramesh, and T. Venkatesan, *Appl. Phys. Lett.* **71** (1997) 2535.
- [33] Yu. P. Sukhorukov, E. A. Gan'shina, B. I. Belevtsev, N. N. Loshkareva, A. N. Vinogradov, K. D. D. Rathnayaka, A. Parasiris, and D. G. Naugle, *J. Appl. Phys.* **91** (2002) 4403.
- [34] Y. Yuzhelevski, V. Markovich, V. Dikovskiy, E. Rozenberg, G. Gorodetsky, G. Jung, D. A. Shulyatev, and Ya. M. Mukovskii, *Phys. Rev. B* **64** (2001) 224428.
- [35] G. H. Rao, J. R. Sun, Y. Z. Sun, Y. L. Zhang, and J. K. Liang, *J. Phys.: Condens. Matter* **8** (1996) 5393.
- [36] X. L. Wang, P. Gehringer, W. Lang, J. Horvat, H. K. Liu, and S. X. Dou, *Solid State Comm.* **117**, 53 (2001).

- [37] A. D. Hernández, C. Hart, R. Escudero, O. Arés, *Physica B* 320 (2002) 64.
- [38] S. Surthi, S. Kotru, R. K. Pandey, P. Fournier, *Solid State Comm.* 125 (2003) 107.
- [39] A. K. Kar, A. Dhar, S. K. Ray, B. K. Mathur, D. Bhattacharya, and K. L. Chopra, *J. Phys.: Condens. Matter* 10 (1998) 10795.
- [40] M. Bibes, Ll. Balcells, J. Fontcuberta, M. Wojcik, S. Nadolski, and E. Jedryka, *Appl. Phys. Lett.* 82 (2003) 928.
- [41] Q. Chen, J. Tao, J. M. Zuo, and J. C. H. Spence, *J. Mater. Res.* 16 (2001) 2959.
- [42] A. de Andrés, M. Garcia-Hernández, and J. L. Martinez, *Phys. Rev. B* 60 (1999) 7328.
- [43] A. Gupta, in *Colossal Magnetoresistance, Charge Ordering and Related Properties of Manganese Oxides*, C. N. R. Rao and B. Raveau (eds.), World Scientific, Singapore (1998), p.189.
- [44] H. Y. Hwang, S-W. Cheong, N. P. Ong, and B. Batlogg, *Phys. Rev. Lett.* 77 (1996) 2041.
- [45] J. E. Evetts, M. G. Blamire, N. D. Mathur, S. P. Isaac, B.-S. Teo, L. F. Cohen, and J. L. MacManus-Driscoll, *Phil. Trans. R. Soc. A* 356 (1998) 1593.
- [46] M. Ziese, *Rep. Progr. Phys.* 65 (2002) 143.
- [47] H. Y. Hwang and S-W. Cheong, in *Colossal magnetoresistive oxides*, Y. Tokura (ed.), Gordon and Breach, Singapore (2000), p.307.

## Figure captions

Figure 1. XRD powder pattern of the inner part of the crystal with nominal composition  $\text{La}_{0.67}\text{Ca}_{0.33}\text{MnO}_3$ . The indicated indexes correspond to lines for cubic perovskite-like unit cell. It is seen that most of the lines are split. To show this more clearly, the region around the (211) reflection is magnified in the inset.

Figure 2. Temperature dependences of the real part,  $\chi'$ , of ac susceptibility for the outer (a) and central (b) parts of the crystal studied. The dependences were recorded (with a 125 Hz ac magnetic field  $H_{ac} = 1 \times 10^{-5}$  T) with increasing temperature after the samples were cooled in zero field.

Figure 3. Temperature dependences of the magnetization of the central part of the sample recorded (in a dc magnetic field  $H_{dc} = 0.2$  mT) with increasing temperature after the sample was cooled in zero field. The inset shows the magnetic-field dependence of the magnetization at  $T = 10$  K.

Figure 4. Temperature dependences of the resistivity of the sample, recorded in zero magnetic field and in fields  $H = 0.5, 1, 2, 3.5$  and  $5$  T. Inset shows a shallow resistance minimum at low temperature. The minimum temperature,  $T''_{min}$ , is about 16 K.

Figure 5. Temperature dependences of the magnetoresistance of the sample, recorded at different magnitudes of applied magnetic field.

Figure 6. Temperature behavior of temperature coefficient of resistance,  $(1/R)(dR/dT)$ , of the sample at zero magnetic field.

Figure 7. Magnetic-field dependences of the magnetoresistance,  $[R(H) - R(0)]/R(0)$ , of the sample at  $T = 4.2$  K and  $68$  K. The dependences were recorded for increasing and subsequently for decreasing applied magnetic field. No significant hysteresis in the curves can be seen.

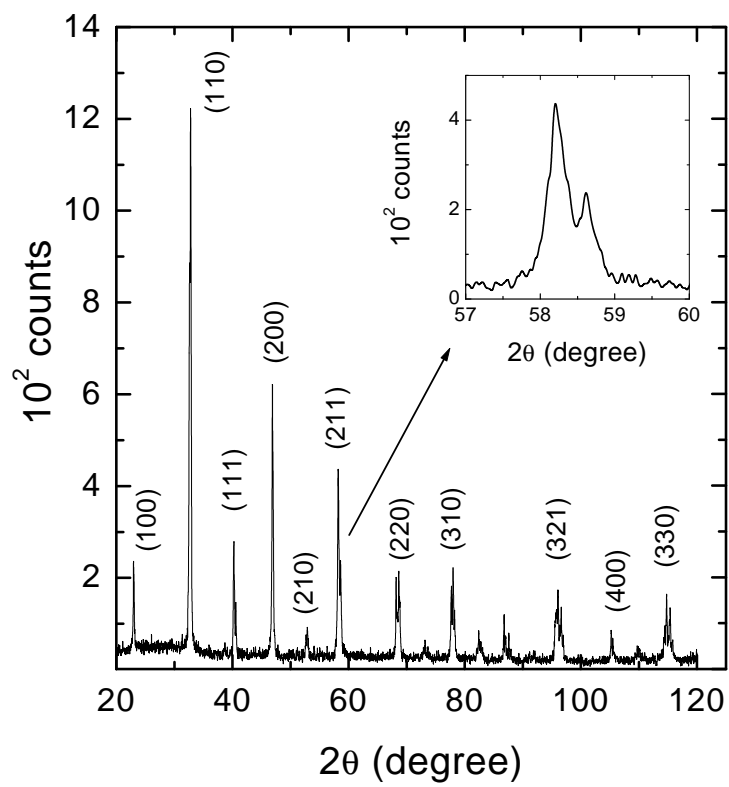


Figure 1 to paper Belevtsev et al.

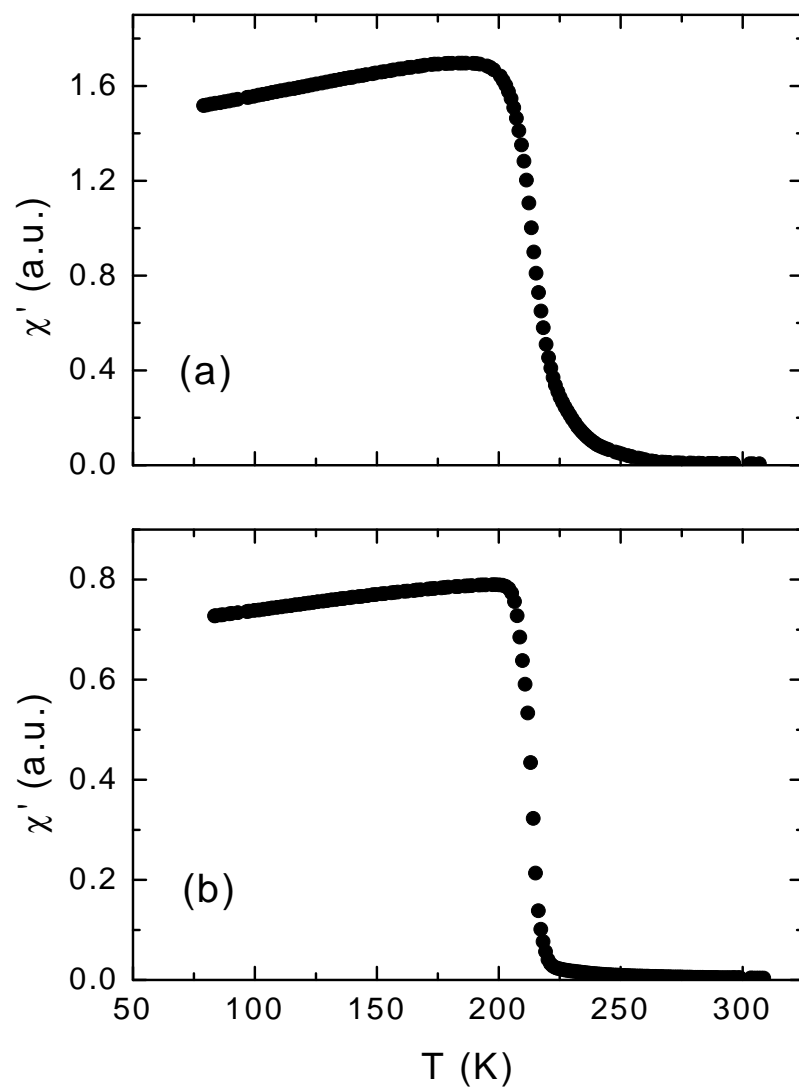


Figure 2 to paper Belevtsev et al.

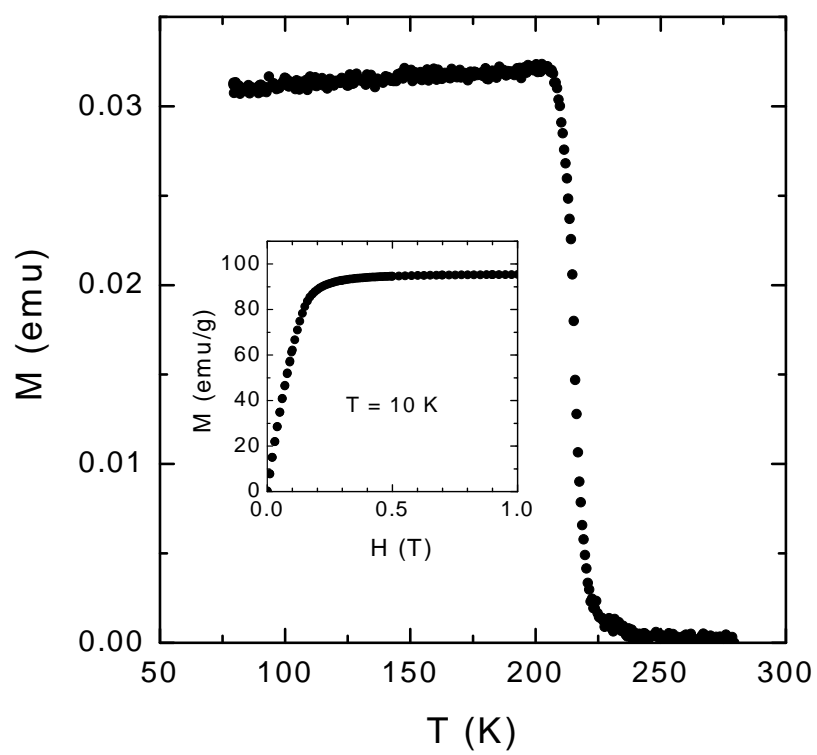


Figure 3 to paper Belevtsev et al.

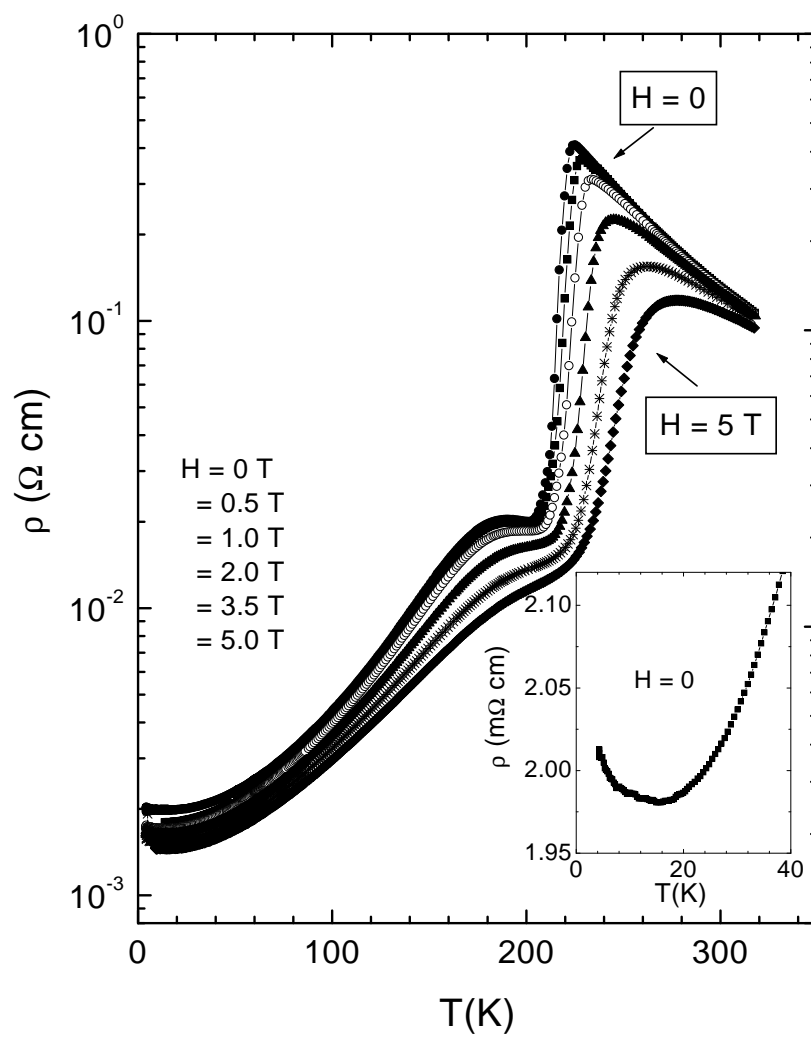


Figure 4 to paper Belevtsev et al.

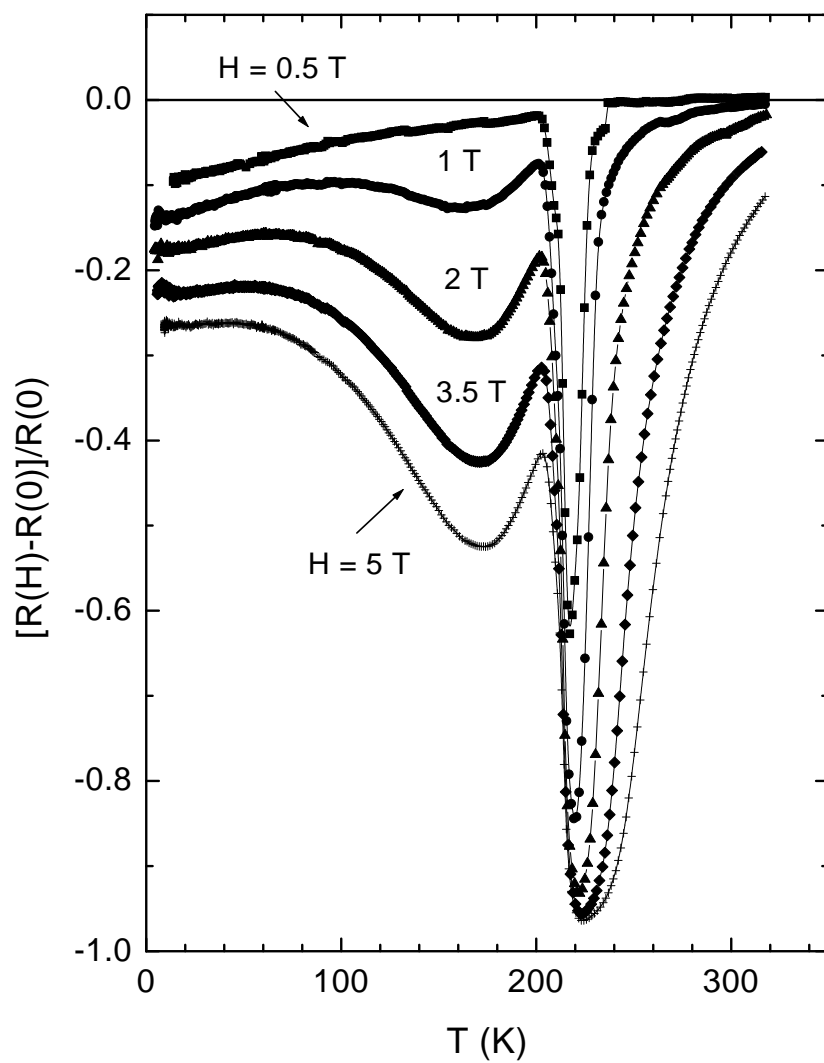


Figure 5 to paper Belevtsev et al.

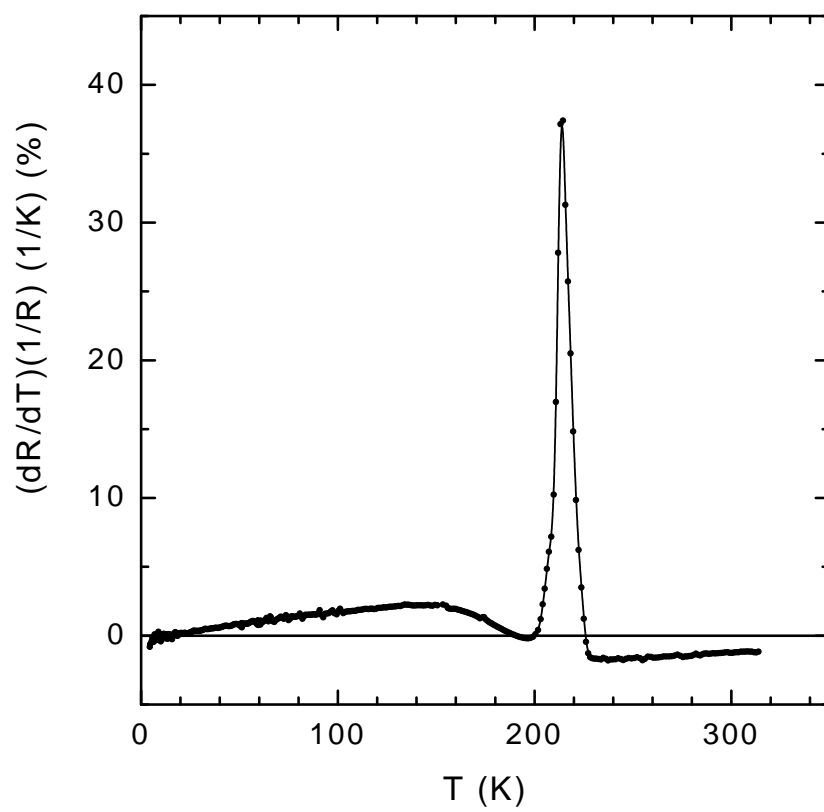


Figure 6 to paper Belevtsev et al.

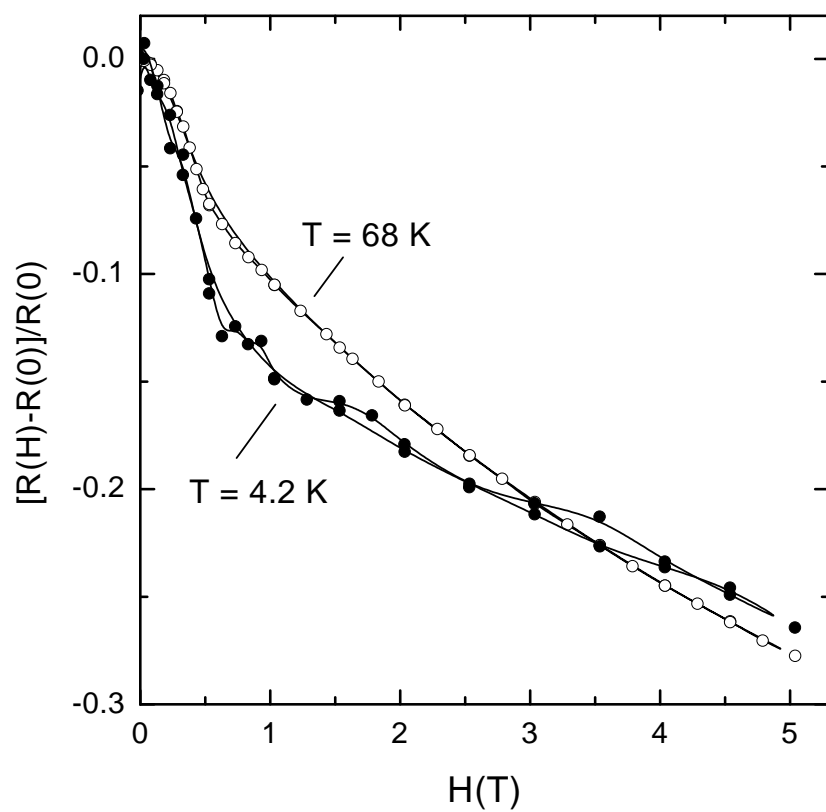


Figure 7 to paper Belevtsev et al.